EUROPEAN SYNCHROTRON RADIATION FACILITY

INSTALLATION EUROPEENNE DE RAYONNEMENT SYNCHROTRON

ESRF	**Experiment title:** Nanoscale reticulation of calcareous biocrystals investigated by 3D Bragg ptychography	**Experiment number**: EV117
Beamline: ID13	**Date of experiment**: from: 1/04/15 to: 7/04/15	**Date of report**: 1/03/20
Shifts: 18	**Local contact(s)**: M. Burghammer	*Received at ESRF:*

Names and affiliations of applicants (* indicates experimentalists):

V. Chamard[1*], C. Chevallard[2,*], P. Godard[2,*], J. Nouet[3,*]

[1]Institut Fresnel, CNRS, Aix-Marseille Université, FST avenue Escadrille Normandie Niemen, 13397 Marseille, France.

2 CEA-LIONS Saclay, France

3 GEOPS Univ Paris Sud, Paris, France

Report:

The proposed experiment aimed at taking advantage of the unique feature of lens-less coherent x-ray imaging in order to clarify the still mysterious mechanisms of bio-crystallization. To this end, we wanted to establish the internal structure of calcareous biocrystals by detailing the spatial relationships between the mineral phase and the occluded organic components, at the very beginning of the mineralization process. According to our previous successful experimental session, the experimental conditions of the ID13 beamline, 3D ptychography imaging in Bragg condition should provide the resolution and field of view needed to shed new light on the bio-mineralization question.

For this experiment, several shell sample from the Pinctada margaritifera specie were prepared and mounted onto a metallic pin. Prior to the experiment, white light optical microscopy and coherent Raman microscopy was performed. The experiment combined nanodiffraction approach with the Frelon camera and 3D Bragg ptychography with the brand new Eiger 4M camera.

The experiment went extremelly well and a large set of high quality data could be acquired, in particular on very early mineralizing prismatic units. However, shortly after the experiment we realized that **the Eiger 4M was not able to record data in a usable fashion as no dedicated trigger signal could be used. Furthermore, a post-experiment synchronization failed to give usable datasets.**

While the ESRF policy does not imply beam compensation for this kind of problem, the ID13 beamline responsible offered several days of inhouse beamtime in june 2016.
This was a very successful beamtime which led to the following publication:

nature materials

ARTICLES

PUBLISHED ONLINE: 10 JULY 2017 | DOI: 10.1038/NMAT4937

Revealing crystalline domains in a mollusc shell single-crystalline prism

F. Mastropietro[1], P. Godard[1†], M. Burghammer[2], C. Chevallard[3], J. Daillant[4], J. Duboisset[1], M. Allain[1], P. Guenoun[3], J. Nouet[5] and V. Chamard[1*]

Biomineralization integrates complex processes leading to an extraordinary diversity of calcareous biomineral crystalline architectures, in intriguing contrast with the consistent presence of a sub-micrometric granular structure. Hence, gaining access to the crystalline architecture at the mesoscale, that is, over a few granules, is key to building realistic biomineralization scenarios. Here we provide the nanoscale spatial arrangement of the crystalline structure within the 'single-crystalline' prisms of the prismatic layer of a *Pinctada margaritifera* shell, exploiting three-dimensional X-ray Bragg ptychography microscopy. We reveal the details of the mesocrystalline organization, evidencing a crystalline coherence extending over a few granules. We additionally prove the existence of larger iso-oriented crystalline domains, slightly misoriented with respect to each other, around one unique rotation axis, and whose shapes are correlated with iso-strain domains. The highlighted mesocrystalline properties support recent biomineralization models involving partial fusion of oriented nanoparticle assembly and/or liquid droplet precursors.

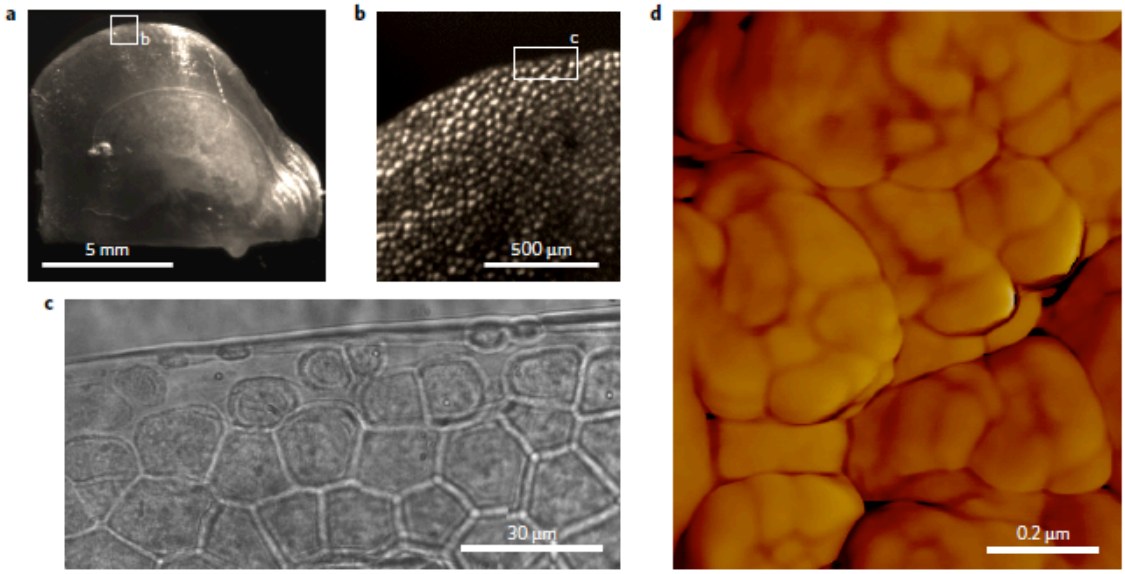

Figure 1 | Structure of *Pinctada margaritifera* shell at different length scales. a–c, Optical micrographs of a juvenile *Pinctada margaritifera*. **a**, The whole shell. **b**, Zoom-in view showing the prism assembly in the vicinity of the growth border. **c**, The shell growth border. Calcite prisms, delimited by thick organic walls, as well as isolated discs, the preliminary form of the prisms, are clearly identified. **d**, Atomic force microscopy images (phase contrast) obtained on the surface of a *Pinctada margaritifera* prism showing the granule assembly, a common structure of many calcifying organisms.

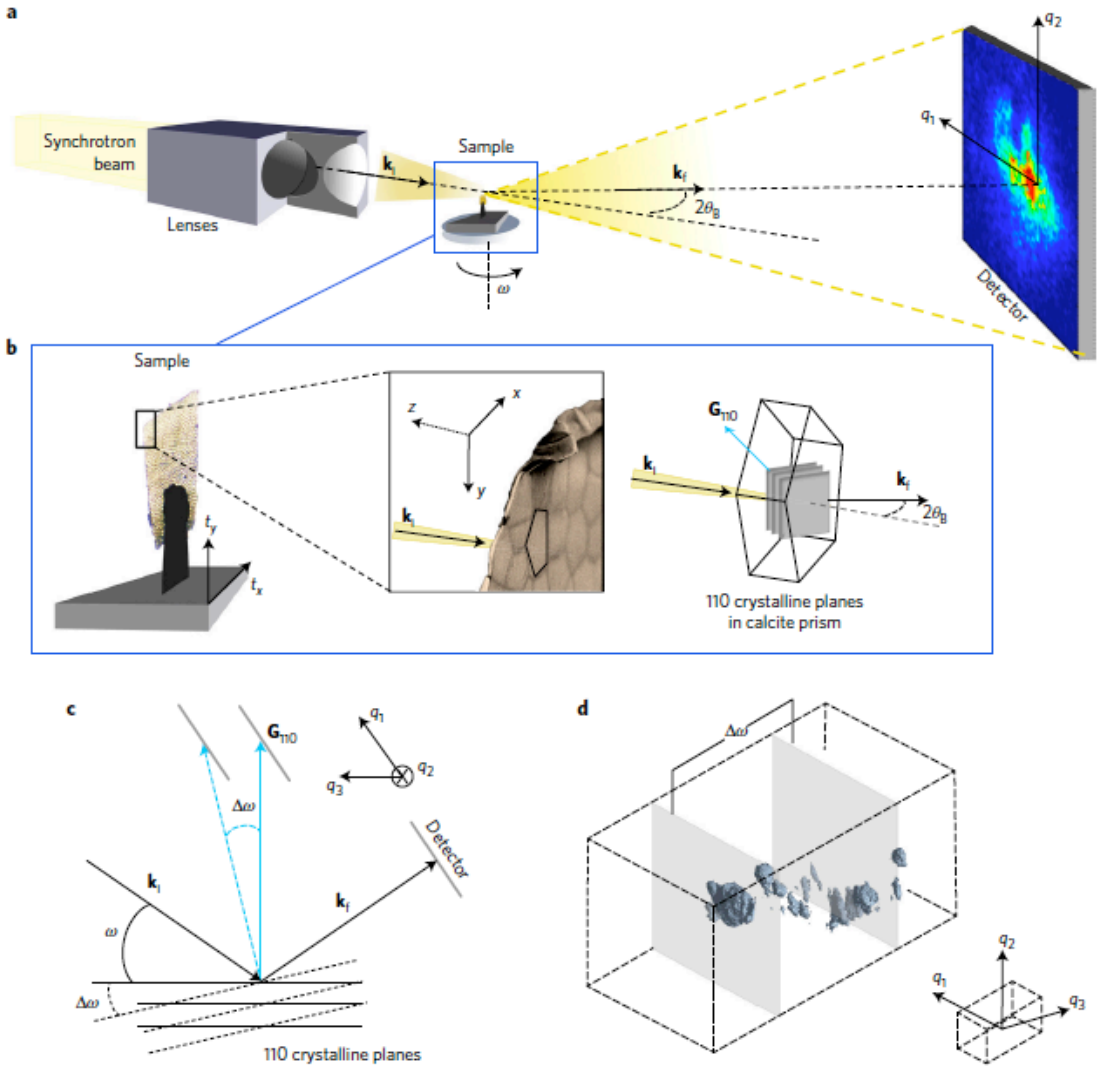

Figure 2 | 3D Bragg diffraction ptychography set-up. a, The sample is placed in the focus of a coherent X-ray nano-beam and oriented in the Bragg diffraction condition in the Laue geometry. The far-field intensity patterns are collected by a 2D detector. **b**, (left) Details of the sample positioning together with the ptychographic translations (t_x and t_y), whose spatial displacements cover the region of interest. (middle) Zoom-in view of the sample where the selected prism is highlighted. The shell thickness is about 1 μm at the border. The (x, y, z) orthogonal laboratory frame is related to the sample, with x and y axes along the surface of the prism and the z axis along the growth direction of the prism. The t_x and t_y ptychography scanning directions are collinear and anti-collinear to the x and y axes, respectively. (right) Chosen 110 Bragg reflection with respect to the prism. The G_{110} Bragg vector lies in the (x, z) plane. **c**, Successive acquisitions of 2D diffraction patterns, obtained by scanning the sample along the incidence angle ω in steps of $\delta\omega$, result in the exploration of the 3D intensity distribution arising from the chosen crystalline family planes. The intensity is recorded as a function of $q = k_f - k_i$, in the 3D detection frame (q_1, q_2, q_3). **d**, Schematic view of the 3D detection frame and isosurface rendition of the 3D intensity distribution integrated over all illumination positions. Two detection planes, separated by n steps along the ω scan, are shown in grey.

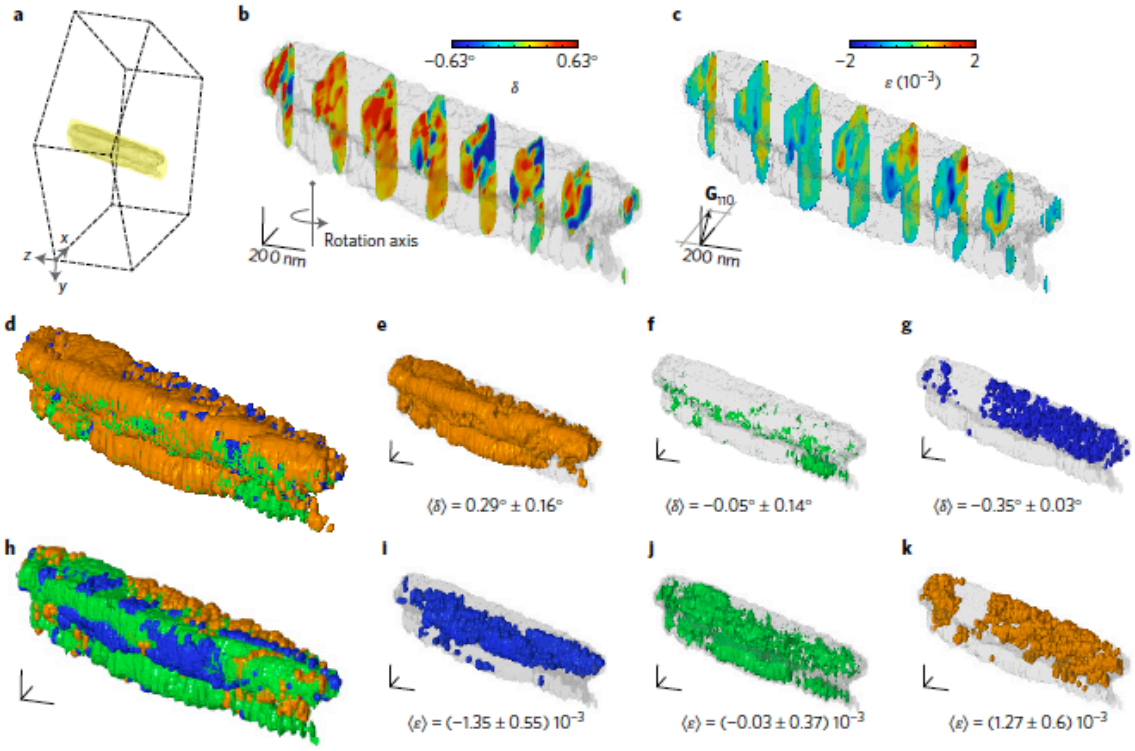

Figure 3 | 3D Bragg ptychography reconstruction. a, Schematic view of the reconstructed volume within the prism (in yellow-grey), embedded into the probed region (yellow cylinder). **b**,**c**, Crystalline rotation (δ) and relative strain (ε) variation maps shown on several planes along the reconstructed volume, corresponding respectively to the rotation of the (110) crystalline planes around the rotation axis shown in **b** and to the relative crystalline displacement along $\mathbf{G}_{110}$. Iso-oriented and iso-strain regions, that is, regions presenting the same rotation or strain value, are discernible. **d**, Same as **b** presented as an isosurface rendition (with respect to δ values) of all iso-oriented crystalline domains. The colours encode the respective rotation angles δ according to the colour scale in **b**. The total retrieved volume corresponds to the one shown in **a**. **e**–**g**, Single iso-oriented crystalline domains, for three rotation angles δ indicated in the figure. **h**, Same as **c** shown as an isosurface rendition (with respect to ε values) of all iso-strain domains. **i**–**k**, Single iso-strain domains, for three relative strains ε indicated in the figure. The length scale is indicated in **b**–**k** and represents 200 nm.

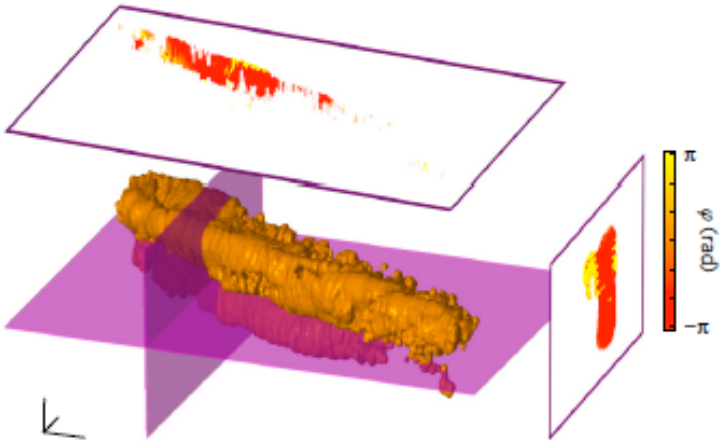

Figure 4 | Crystalline coherence in the iso-oriented domain. 2D cuts of the retrieved phase map φ extracted for the iso-oriented domain of Fig. 3e. This quantity is related to the crystalline coherence: abrupt changes in the phase value correspond to breakdown of the crystalline continuity. On average, the phase shift is about 4.2 rad, corresponding to a displacement of about 0.16 nm, that is, ≈2/3 of the (110) lattice spacing. The indicated length scale represents 200 nm.